Two-photon magnetoabsorption of ZnTe, CdTe, and GaAs

Ch. Neumann and A. Nöthe
Institut für Physik, Universität Dortmund, Postfach 50 05 00, D-4600 Dortmund 50, Federal Republic of Germany

N. O. Lipari
IBM Thomas J. Watson Research Center, P.O. Box 218, Yorktown Heights, New York 10598
(Received 20 May 1987)

Two-photon magnetoabsorption measurements of $2P$ excitons in ZnTe, CdTe, and GaAs are presented. The measurements are carried out in Faraday ($\mathbf{k}\|\mathbf{B}$) and Voigt ($\mathbf{k}\perp\mathbf{B}$) configuration in fields up to 7 T. Besides a Zeeman splitting and a diamagnetic shift, a drastic enhancement of the two-photon oscillator strength is detected. This enhancement is due to the magnetic-field-induced compression of the wave function. The energies and the wave functions are calculated with use of an effective-mass Hamiltonian which includes the degeneracy of the valence band. From a fit of the calculated eigenvalues to the experimental results all relevant mass parameters and g values (m_e^*, γ_1, γ_2, γ_3, g_c, κ, q) are deduced. The large number of magnetic components allows a consistent and precise determination of all relevant parameters.

I. INTRODUCTION

The band structure of direct-band-gap semiconductors in the vicinity of the center of the Brillouin zone is properly described by a few parameters: the band-gap energy, the band masses, and the g values of conduction and valence bands. There are many experimental methods to determine different parts of this parameter set, such as cyclotron resonance,[1-11] magnetoreflection measurements,[12-14] one-photon magnetoabsorption,[15,16] Faraday rotation,[17] Raman scattering,[18] etc. A disadvantage of these methods is that each experiment can only determine a part of the parameter set. Furthermore, for the analysis of the experiments in most cases additional assumptions have to be made. In contrast to this, two-photon magneto-optics of P excitons allows the determination of the complete parameter set. This method has been already successfully applied to ZnSe.[19] Because of the large number of states (24) the $2P$-exciton spectra contain so much experimental information that a precise determination of all relevant parameters is possible, since P excitons are completely described by these parameters. For the analysis of S-exciton spectra one needs a much more sophisticated theoretical treatment with some additional parameters. Owing to the more extended wave function of P excitons compared to the $1S$ exciton, polaron corrections can be done for electron and hole separately. Because of the vanishing wave function at the origin there are no central-cell corrections, which are important for S excitons. Furthermore P excitons in zinc-blende-type semiconductors are dipole forbidden, i.e., there is no exciton-photon interaction. This fact simplifies the analysis considerably, because the polariton dispersion does not have to be considered. As was shown by Uihlein and Feierabend[20] in the case of ZnSe, magneto-optical investigations of the $1S$ excitons have to take exciton-photon interaction into account. In contrast to S-exciton data the analysis of the P-exciton data is much easier and clearer. We calculate the energies of the exciton states as a function of the magnetic field using the effective-mass Hamiltonian from Altarelli and Lipari.[21] The Hamiltonian includes the degeneracy of the valence bands, the Coulomb interaction between electrons and holes, and the external magnetic field. The calculation for the P excitons is straightforward and the determination of the parameters is possible without the use of additional assumptions. Another feature which makes the investigation of P excitons very interesting is the magnetic field dependence of their oscillator strength. For P excitons this effect is one order of magnitude larger than for S excitons. In this paper we report the P exciton spectra of ZnTe, CdTe, and GaAs and the analysis of their magnetic field dependence.

The paper is organized as follows. After this introduction the experimental setup is described briefly. In the following theoretical section we present at the beginning (Sec. III A) the Hamiltonian for excitons originating from a degenerate Γ_8 valence band and our method of solution. In Sec. III B the two-photon selection rules are given and in Sec. III C we derive an expression for the two-photon oscillator strength of P excitons. In Sec. IV we present our measurements of the P-exciton spectra of ZnTe, CdTe, and GaAs. The parameters which are determined from the spectra are compared to the results of other experiments.

II. EXPERIMENT

The two-photon magnetoabsorption measurements on the P-exciton fine structure of ZnTe, CdTe, and GaAs were carried out with the experimental setup shown in Fig. 1.

The two light sources for the two-photon process are a cw dye laser and a transverse-excitation atmospheric (TEA) CO_2 laser. Different dyes are used to get the required tuning ranges for the investigation of ZnTe,

CdTe, and GaAs. Rhodamine-560 with a tuning range from 535 to 580 nm and Styryl-9 with a tuning range from 790 to 890 nm are suitable. The dye laser is pumped by an argon-ion laser and is tuned by a Lyot filter, which allows a spectral resolution better than 0.1 meV. The TEA CO_2 laser has a repetition rate of 10 Hz and a maximum output power of 3 MW in a 150-ns pulse. The beam is focused onto the crystal to an area of 1 mm^2, which results in a maximum intensity of 300 MW/cm^2. The photon energy of the CO_2 laser (0.117 eV) is relatively small, which has two advantages. On the one hand the spectral range for two-photon measurements is extended to lower energies. On the other hand one gets a strong enhancement of the two-photon absorption because the dye-laser photon is nearly resonant with the intermediate state. This enhancement allows one to carry out two-photon absorption measurements with crystals thinner than 1 mm.

The cw dye laser is chopped to get pulses of about 20 μs and the CO_2 laser is synchronized to the chopper. The polarization states of the laser beams can be varied automatically by rotating half-wave or quarter-wave retardation plates. The two laser beams are superimposed onto the crystal, which is mounted in a cryostat. For the measurements in Faraday and Voigt configurations two different helium cryostats with superconducting coils are used. The first one contains a 9 T solenoid. The crystal is thermally coupled to the liquid helium by low-pressure helium gas. This cryostat is used for the measurements in Faraday configuration. For the measurements in Voigt configuration it is advantageous to use the second cryostat which contains a 7-T split coil. In this cryostat the crystal is immersed in liquid helium.

The intensity of the CO_2 laser is measured by a Hg-Cd-Te detector with a rise time of 1 ns and a high responsivity at 10.6 μm. The intensity of the dye laser is detected by a photomultiplier tube (S20) or a photodiode (RCA C30950G). The short two-photon signal Δ is separated from the long dye laser pulse by differentiation. The digitized signal is then normalized to the laser intensities and analyzed by an on-line calculator. The wavelength of the dye laser can be measured with a 1-m monochromator and monitored by an optical-multichannel-analyzer (OMA-II) system which is calibrated with the use of mercury and neon emission lines. The spectral resolution is determined by the bandwidth of the dye laser, which is better than 0.1 meV.

III. THEORY

In Sec. III A we will present a magnetic field Hamiltonian for the excitons originating from a Γ_8 valence band and the methods of solution. In Sec. III B we will discuss the two-photon selection rules. In the last part (Sec. III C) we will consider the two-photon oscillator strength.

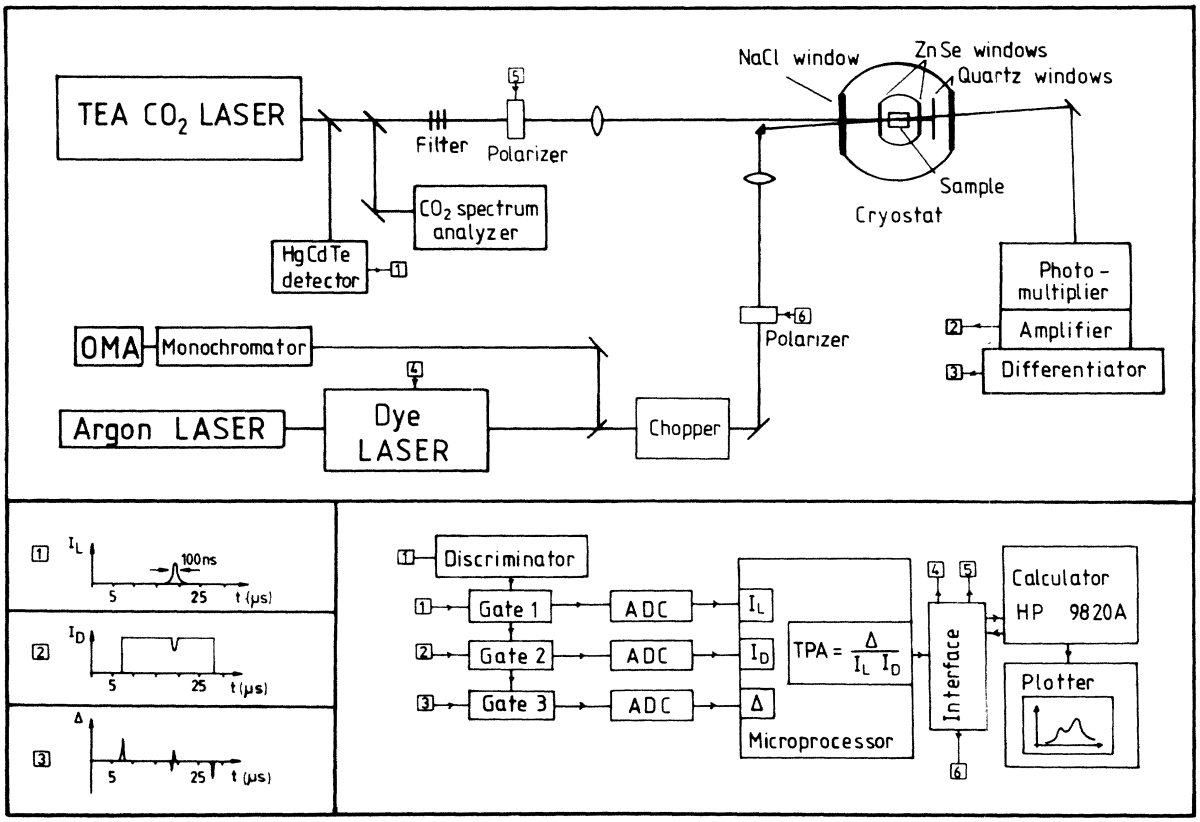

FIG. 1. Experimental setup for two-photon magnetoabsorption measurements.

A. The magnetic field Hamiltonian

The calculation of the eigenvalues and eigenstates of the P-exciton multiplet is done within the framework of the effective-mass theory. We neglect all terms of higher order than k^2, which is valid in the vicinity of the Γ point. We also neglect terms linear in k because they are small. Our measurements on ZnTe show that the energetic splitting due to k-linear terms is smaller than 10 μeV. From a recent calculation of Cardona *et al.*[22] we know the k-linear term of CdTe and GaAs to be of the same order of magnitude as in ZnTe or even smaller.

The problem of excitons originating from a degenerate Γ_8 valence band has been treated in a series of papers[23–26] by Baldereschi, Lipari, and Altarelli. Their method of solution gives eigenvalues and eigenstates for excitons of degenerate bands for any value of an external magnetic field, which are correct within the experimental accuracy of 10 μeV. The method uses the formalism of irreducible spherical tensor operators, which enables the analytical calculation of the angular dependent parts of the Hamiltonian. The Hamiltonian consists of three parts; one independent of the magnetic field, the second linear, and the third quadratic in the magnetic field:

$$
\begin{aligned}
&H = H_0 + H_1(B) + H_2(B^2) \ , \\
&H_0 = \frac{p^2}{\hbar^2} - \frac{2}{r} - \frac{\mu}{9\hbar^2}\mathbf{P}^{(2)}\cdot\mathbf{J}^{(2)} + \frac{\delta}{9\hbar^2}[(\mathbf{P}^{(2)}\times\mathbf{J}^{(2)})^{(4)}_4 + \sqrt{14/5}(\mathbf{P}^{(2)}\times\mathbf{J}^{(2)})^{(4)}_0 + (\mathbf{P}^{(2)}\times\mathbf{J}^{(2)})^{(4)}_{-4}] \ , \\
&H_1(B) = \mu_B B(\gamma_e - \gamma_1)L_z + \mu_B B g_c S_z - 2\mu_B B(\kappa + \tfrac{9}{4}q)J_z - \tfrac{2}{5}\mu_B B q J^{(3)}_0 \\
&\quad - \frac{i}{9\hbar^2}(\gamma_e+\gamma_1)\mu\sqrt{5/6}\mu_B B\{[(\mathbf{R}^{(1)}\times\mathbf{P}^{(1)})^{(1)}\times\mathbf{J}^{(2)}]^{(1)}_0 - \sqrt{3}[(\mathbf{R}^{(1)}\times\mathbf{P}^{(1)})^{(2)}\times\mathbf{J}^{(2)}]^{(1)}_0\} \\
&\quad - \frac{i}{9\hbar^2}(\gamma_e+\gamma_1)\delta\sqrt{2/5}\mu_B B\{[(\mathbf{R}^{(1)}\times\mathbf{P}^{(1)})^{(2)}\times\mathbf{J}^{(2)}]^{(3)}_0 + \sqrt{2}[(\mathbf{R}^{(1)}\times\mathbf{P}^{(1)})^{(1)}\times\mathbf{J}^{(2)}]^{(3)}_0\} \\
&\quad - \frac{i}{9\hbar^2}(\gamma_e+\gamma_1)\delta\mu_B B\{[(\mathbf{R}^{(1)}\times\mathbf{P}^{(1)})^{(2)}\times\mathbf{J}^{(2)}]^{(4)}_4 - [(\mathbf{R}^{(1)}\times\mathbf{P}^{(1)})^{(2)}\times\mathbf{J}^{(2)}]^{(4)}_{-4}\} \ , \\
&H_2(B^2) = (\gamma_e+\gamma_1)^2\mu_B^2 B^2\left[\frac{1}{6\hbar^2}(r^2 - \tfrac{1}{2}\sqrt{2/3}R^{(2)}_0) + \frac{\mu}{108\hbar^2}\mathbf{R}^{(2)}\cdot\mathbf{J}^{(2)}\right. \\
&\qquad + \frac{1}{9\hbar^2}\sqrt{2/7}\left[\frac{7\mu}{12} - \frac{\delta}{5}\right](\mathbf{R}^{(2)}\times\mathbf{J}^{(2)})^{(2)}_0 + \frac{1}{27\hbar^2}\sqrt{2/3}\left[\frac{\mu}{4} - \frac{3\delta}{10}\right]r^2 J^{(2)}_0 \\
&\qquad \left. - \frac{\delta}{36\hbar^2}[(\mathbf{R}^{(2)}\times\mathbf{J}^{(2)})^{(4)}_{-4} - \sqrt{2/35}(\mathbf{R}^{(2)}\times\mathbf{J}^{(2)})^{(4)}_0 + (\mathbf{R}^{(2)}\times\mathbf{J}^{(2)})^{(4)}_4]\right] \ ,
\end{aligned}
\tag{1}
$$

with

$$
\mu = \frac{6\gamma_3 + 4\gamma_2}{5(\gamma_e+\gamma_1)} \ , \quad \delta = \frac{\gamma_3 - \gamma_2}{(\gamma_e+\gamma_1)} \ . \tag{2}
$$

The Hamiltonian (1) is written in units of the effective Rydberg energy and the exciton Bohr radius:

$$
R_{\text{eff}} = \frac{1}{(\gamma_e+\gamma_1)\epsilon^2}R_H \ , \quad a_{\text{ex}} = (\gamma_e+\gamma_1)\epsilon a_B \ , \tag{3}
$$

where γ_e is the reciprocal of the electron mass m_e^*. The parameters γ_1, γ_2, and γ_3 are the Luttinger parameters of the Γ_8 valence band and ϵ is the dielectric constant. The g value of the conduction band is g_c. The parameters κ and q are the isotropic and anisotropic g values of the valence band, respectively.

For the calculation of the eigenvalues we use the following Ansatz for the eigenfunctions:

$$
\Psi_i(\mathbf{r}) = \sum_{L,F,M_F} f_{i,L,F,M_F}(r)\ |L,J,F,M_F\rangle\ |S,M_S\rangle \ , \tag{4}
$$

where i plays the role of a principal quantum number. As parity is still a good quantum number, the sum over L includes only either all even or all odd integers. For P excitons we have to include states with odd angular momentum L. F is the angular momentum which is composed of the hole spin J and the envelope angular momentum L. The coupling of L and J is due to the degeneracy of the Γ_8 valence band. Since for P excitons there is no coupling between the electron spin S and the angular momentum F, the electron spin can be separated. The electron spin only doubles the number of states and gives rise to a splitting of the states according to the g value g_c. M_F is the z component of the angular momentum F and is a good quantum number in the spherical approximation ($\delta=0$). The complete Hamiltonian mixes wave functions with $\Delta M_F = 0, \pm 4$, but the mixing is quite small. Therefore the states can still be characterized by M_F and M_S. Their sum is the total quantum number $M_{\text{tot}} = M_F + M_S$. The angular part of the eigenvalue problem can be eliminated analytically by using the Ansatz (4) and the Wigner-Eckart theorem together with $3j$, $6j$, and $9j$ symbols.[27] One gets a system of radial differential equations of the order N_1, where N_1

is the number of terms in the expansion for the angular functions. We have used two different numerical methods in order to solve this system of differential equations. The first method uses a finite-element technique. Here the argument of the radial functions $f_{i,L,F,M_F}(r)$ is regarded as a discrete variable running through N_2 points within an interval given by the origin and a cutoff radius. Thus the wave functions and the differential operators are represented by N_2-dimensional vectors and $N_2 \times N_2$ matrices, respectively.[27] In this way the problem is transformed into the diagonalization of a secular determinant of the order $N_1 N_2$. The eigenvalues are calculated by a computer program which treats the Hamiltonian in the axial approximation including angular wave functions with $L=1$ and $L=3$. We have used this program for the analysis of the ZnTe measurements and have achieved satisfactory numerical accuracy using $N_2=200$. For CdTe and GaAs the restriction to $L=1$ and $L=3$ is no longer sufficient because of the smaller values for the band masses and the exciton binding energies. For these materials we have used the second method, in which the radial wave functions are expanded into a number of N_2 exponentials. The analytical determination of the angular-dependent matrix elements and the solution of the secular determinants of the order $N_1 N_2$ have been done by a computer program which was developed by Lipari and Altarelli.[21] The program allows one to take into account angular functions with any angular momentum L. A total of 15 exponentials was sufficient for a relative accuracy of 10^{-6}. For the hydrogen problem and for ZnTe we have tested that both programs yield the same results for the eigenvalues and eigenfunctions.

The computed eigenvalues are functions of the Rydberg energy, the effective mass m_e^*, the Luttinger parameters $\gamma_1, \gamma_2, \gamma_3$, and the g values of electron and hole. From a fit of the calculated eigenvalues to the measured $2P$-exciton spectra it is possible to determine these parameters with great accuracy. The fitting procedure is facilitated by the fact that the number of experimental data considerably exceeds the number of parameters. In fact the Zeeman splitting of the $2P$-exciton system depends so critically on the choice of the effective-mass parameters that a good agreement between experiment and theory is not only a rigorous test for the reliability of the mass parameters but also a proof for the validity of the effective-mass Hamiltonian (1).

B. Two-photon absorption selection rules

The two-photon selection rules result from a combination of two one-photon absorption processes. For electric dipole transitions the selection rules $\Delta L = \pm 1$ and $\Delta M = 0$ or ± 1 are valid for the absorption of one photon. Therefore one gets $\Delta L = 0$ or ± 2 and $\Delta M = 0, \pm 1$, or ± 2 for the absorption of two photons. Depending on the polarization directions of both lasers a selective excitation of the magnetic substates is possible. In Faraday configuration ($\mathbf{k} \| \mathbf{B}$), circularly polarized light is used which leads to transitions into states with the total magnetic quantum number $M_{\text{tot}} = 0$ or ± 2. It should be noted that the selection rules only depend on the helicity of the photons with respect to the magnetic field. With the use of two circularly polarized beams of opposite helicity one can excite states with $M_{\text{tot}} = 0$. With two beams of the same helicity, transitions into magnetic substates with $M_{\text{tot}} = \pm 2$ are possible. Measurements in Voigt configuration ($\mathbf{k} \perp \mathbf{B}$) with linearly polarized light allow the observation of states with $M_{\text{tot}} = 0, \pm 1$, and ± 2. The polarization axis of linearly polarized light is either parallel (π) or perpendicular (σ) to the magnetic field. States with $M_{\text{tot}} = \pm 1$ are excited by a combination of π- and σ-polarized light. If both polarizations are parallel to the magnetic field, transitions to $M_{\text{tot}} = 0$ are possible. If both are perpendicular to the magnetic field, transitions to $M_{\text{tot}} = 0$ and ± 2 are possible. The different combinations are listed in Table I.

C. Two-photon oscillator strength

For the calculation of the two-photon oscillator strength we will only consider contributions from the Γ_8 valence band and the Γ_6 conduction band, which is justified by our special experimental setup. Due to the small photon energy of the CO_2 laser the dye laser energy is nearly resonant for transitions into states which are the intermediate states of the two-band model. This allows one to neglect contributions of other bands because of the much greater resonance denominators. The main points of the following derivation are attributable to Mahan.[29] The transition probability for the two-photon process is given by

$$W = \frac{2\pi}{\hbar} \sum_{i,f} S_f(E) \, | \, V_{if} \, |^2 \, ; \tag{5}$$

$S_f(E)$ is the final density of states and V_{if} is the matrix element between initial and final state and is given by

$$V_{if} \propto \sum_l \left[\frac{\langle f \, | \, \boldsymbol{\varepsilon}_1 \cdot \mathbf{p} \, | \, 1 \rangle \langle l \, | \, \boldsymbol{\varepsilon}_2 \cdot \mathbf{p} \, | \, i \rangle}{E_l - E_i - \hbar\omega_2} + \frac{\langle f \, | \, \boldsymbol{\varepsilon}_2 \cdot \mathbf{p} \, | \, l \rangle \langle l \, | \, \boldsymbol{\varepsilon}_i \cdot \mathbf{p} \, | \, i \rangle}{E_l - E_i - \hbar\omega_1} \right] , \tag{6}$$

where $\boldsymbol{\varepsilon}_1$ and $\boldsymbol{\varepsilon}_2$ are the polarization vectors and $\hbar\omega_1$ and

TABLE I. Selection rules for the two-photon absorption process. The polarizations are given with respect to the magnetic field.

Polarization state		M_{tot}
$\mathbf{k} \| \mathbf{B}$	$\sigma_+ \sigma_+$	2
	$\sigma_+ \sigma_-$	0
	$\sigma_- \sigma_+$	0
	$\sigma_- \sigma_-$	−2
$\mathbf{k} \perp \mathbf{B}$	$\sigma\sigma$	0, ±2
	$\sigma\pi$	±1
	$\pi\sigma$	±1
	$\pi\pi$	0

$\hbar\omega_2$ the photon energies of the two photons. In the two-band model the summation over l is a summation over all allowed exciton states with energies $E=E_g+E_n$, where E_n is the binding energy of an exciton state. The first matrix element was calculated by Elliott:[30]

$$\langle l \mid \varepsilon_\alpha \cdot \mathbf{p} \mid i \rangle = \sqrt{V}\, \Psi_\lambda^*(0) \langle c \mid \varepsilon_\alpha \cdot \mathbf{p} \mid v \rangle \ , \tag{7}$$

where $\Psi_\lambda^*(0)$ is the exciton wave function of state λ at $r=0$ and $\langle c \mid \varepsilon_\alpha \cdot \mathbf{p} \mid v \rangle$ is evaluated between Bloch functions. The second matrix element describes the change of the exciton envelope due to the second photon and can be written as

$$\langle f \mid \varepsilon_\beta \cdot \mathbf{p} \mid l \rangle = \frac{m_e}{\mu} \int d^3r\, \Psi_\nu^*(r) \varepsilon_\beta \cdot \mathbf{p} \Psi_\lambda(r) \ . \tag{8}$$

where μ is the reduced exciton mass and ν represents all quantum numbers of the final state. With the definition

$$I_\nu(\alpha,\beta) = \int d^3r\, \Psi_\nu^*(r) \varepsilon_\beta \cdot \mathbf{p} \sum_\lambda \frac{\Psi_\lambda(r)\Psi_\lambda^*(0)}{E_\lambda + E_G - \hbar\omega_\alpha} \ , \tag{9}$$

V_{if} can be written as

$$V_{if} \propto [\langle c \mid \varepsilon_1 \cdot \mathbf{p} \mid v \rangle I_\nu(1,2) + \langle c \mid \varepsilon_2 \cdot \mathbf{p} \mid v \rangle I_\nu(2,1)] \ . \tag{10}$$

If the values k_1 and k_2,

$$k_\alpha = \left[\frac{R_{\text{eff}}}{E_G - \hbar\omega_\alpha} \right]^{1/2} \ ,$$

are small ($k_1, k_2 \leq 0.5$) one can use an approximate formula for I_ν,

$$I_\nu(\alpha,\beta) = -i \frac{\hbar k_\alpha^2}{R_{\text{eff}}} [\varepsilon_\beta \cdot \nabla \Psi_\nu(r)]_{r=0} \ . \tag{11}$$

The result (11) depends on the first derivative of the exciton wave function at $r=0$. With this approximation Eq. (5) becomes

$$W_{m_s,m_F} \propto \left| \sum_{m,m_L,m_J} \frac{\varepsilon_{1-m}^{(1)} \cdot \varepsilon_{2-m_L}^{(1)}}{E_G - \hbar\omega_1} \delta_{m_L+m_J,m_F} A_{m_L}^P \times C_G [\nabla_r \Psi_{m_L,m_J}(r)]_{r=0} + (1 \leftrightarrow 2) \right|^2 \ . \tag{12}$$

The Clebsch-Gordan coefficients $C_G = \langle \frac{1}{2}\, \frac{3}{2}\, m_S\, m_J \mid 1\, m \rangle$ arise from the matrix elements between the band functions. The factor $A_{m_L}^P$ is the P-like part of the wave function and takes into account the selection rules for dipole transitions. For the polarization vectors of the photons we have taken the irreducible spherical tensor operators which are defined as follows:

$$\varepsilon^{(1)}(\sigma_+) = \begin{bmatrix} 0 \\ 0 \\ 1 \end{bmatrix}, \quad \varepsilon^{(1)}(\sigma_-) = \begin{bmatrix} 1 \\ 0 \\ 0 \end{bmatrix} ,$$

$$\varepsilon^{(1)}(\sigma) = \sqrt{1/2} \begin{bmatrix} 1 \\ 0 \\ 1 \end{bmatrix}, \quad \varepsilon^{(1)}(\pi) = \begin{bmatrix} 0 \\ 1 \\ 0 \end{bmatrix} .$$

The oscillator strength (12) depends strongly on the magnitude of the magnetic field. The magnetic field causes a compression of the exciton wave function, which yields a strong increase of the first derivative of the wave function at the origin. This is a unique feature of P excitons.[31] The oscillator strength of S excitons depends on the value of the wave function at the origin, which depends much less on the magnetic field.

IV. EXPERIMENTAL RESULTS AND DISCUSSIONS

A. ZnTe

The $2P$-exciton spectra of ZnTe in the field-free case exhibits four states, each of them multiple degenerate.[32] This degeneracy is lifted by an external magnetic field. Figure 2 shows the $2P$-exciton spectra at 5 T for eight polarization combinations in Faraday and Voigt configurations. The selective excitation of states with different quantum number M_{tot} enables the unambigous assignment of the absorption peaks. Figure 3 shows a comparison of the magnetic field dependence of the absorption peaks to the calculated eigenvalues. The eigenvalues are computed using the following parameters which give the best fit to the experimental data:

$$m_e^* = (0.116 \pm 0.003) m_0, \quad R_{\text{eff}} = 14.1 \pm 0.2 \text{ meV} \ ,$$

$$\gamma_1 = 4.07 \pm 0.10, \quad E_g = 2.3945 \pm 0.0002 \text{ eV} \ ,$$

$$\gamma_2 = 0.78 \pm 0.14, \quad g_c = -0.78 \pm 0.06 \ ,$$

$$\gamma_3 = 1.59 \pm 0.11, \quad \kappa = 0.27 \pm 0.05 \ .$$

Especially γ_1 and m_e^* can be determined with great accuracy because of the critical dependence of the splittings on these two parameters. In Table II we give a comparison between our values and the results of other authors. Our value for the conduction-band mass is in perfect agreement with the value of Dean *et al.*,[33] which they derive from conduction band to acceptor luminescence. The cyclotron resonance measurements of Clerjaud *et al.*[1] yield a slightly greater mass which is within the experimental errors. The results of Nahory and Fan[34] and Vanecek and Klier[35] are gained from photoconductivity measurements. Both groups use an isotropic model and assume an average value for the heavy-hole mass to get their value for the conduction band mass. Because of the relatively large anisotropy of the heavy-hole mass in ZnTe this approximation is not valid.

Our Luttinger parameters are in good agreement with the infrared absorption and Raman scattering data of Nakashima *et al.*[18] Also the cyclotron resonance measurements of Stradling[2] are consistent with our parameters except that his analysis yields a smaller anisotropy.

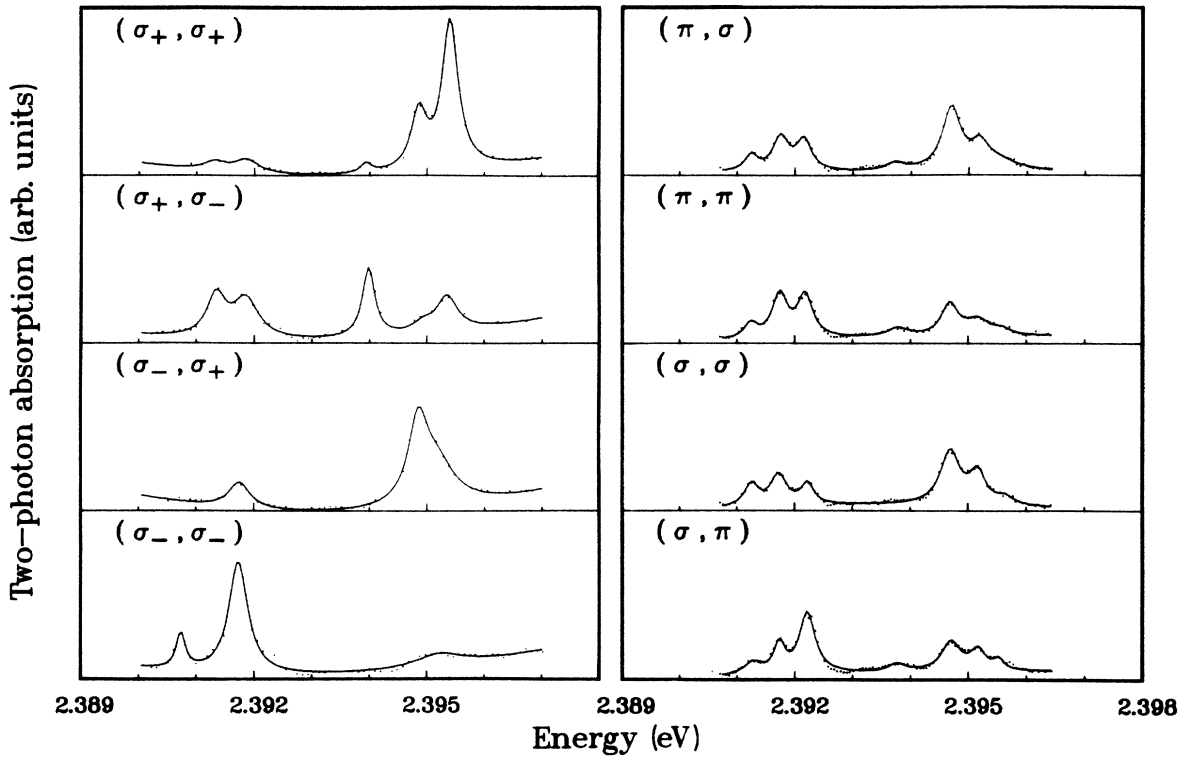

FIG. 2. 2*P*-exciton fine structure of ZnTe at 5 T for the eight different polarization states of the two beams in Faraday (left) and in Voigt configuration (right). The first sign refers to the polarization of the dye laser, the second to the polarization of the TEA CO_2 laser. The polarization is defined with respect to the magnetic field.

There are slight differences to the measurements of Maier *et al.*[12] and Venghaus and Jusserand[13] on *S* excitons. These differences could be due to the fact that in the analysis of *S* exciton spectra, exciton-photon interaction, exciton-phonon interaction, and central-cell corrections have to be taken into account, which makes the analysis more difficult and leads to additional parameters. Furthermore the *S*-exciton spectra are reflection spectra so that a Kramers-Kronig transformation is needed to get the energy values of the resonances.

In our analysis we have neglected *k*-linear terms. In order to justify this approximation we have made a direct measurement of the *k*-linear term by rotating the crystal by 180° about an axis which is not a twofold rotation axis of the crystal. Because of time-reversal symmetry the energy of an exciton with wave vector **k** and spin up is equal to the energy of an exciton with $-\mathbf{k}$ and spin down:

$$E(\mathbf{k})|\uparrow\rangle = E(-\mathbf{k})|\downarrow\rangle \ .$$

In a magnetic field the spin up states and the spin

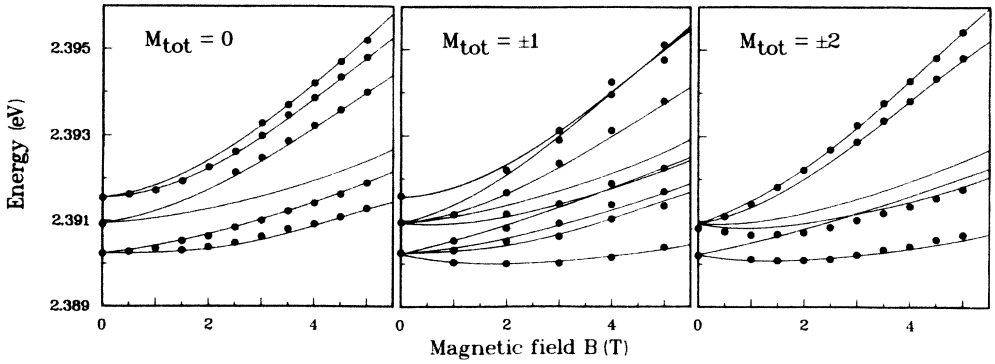

FIG. 3. Magnetic field dependence of the 2*P* multiplet in ZnTe: lines, results of the calculations; dots, experimental peak positions.

TABLE II. Fundamental parameters of ZnTe.

	m_e^*/m_0	γ_1	γ_2	γ_3	R_{eff} (meV)	g_c	κ
This work	0.116	4.07	0.78	1.59	14.1	−0.78	0.27
Dean *et al.*[a]	0.116						
Clerjaud *et al.*[b]	0.122						
Nahory and Fan[c]	0.09						
Vanecek and Klier[d]	0.107						
Nakashima *et al.*[e]		4.2	0.91	1.54			
Stradling[f]		4.0	1.15	1.29			
Maier *et al.*[g]		3.9	0.6	0.9	12.8	−0.65	0.14
Venghaus and Jusserand[h]		3.9	0.83	1.30	12.8	−0.6	0.0

[a] Reference 33.
[b] Reference 1.
[c] Reference 34.
[d] Reference 35.
[e] Reference 18.
[f] Reference 2.
[g] Reference 12.
[h] Reference 13.

down states are separated. We have measured the $M_F=\frac{5}{2}$, $M_S=-\frac{1}{2}$ state at 5 T for $\mathbf{k}$ and $-\mathbf{k}$ by rotating the crystal by 180°. The shift of the absorption line was smaller than 10 μeV, which is the minimal detectable shift in our experimental setup. This leads to an upper limit of the k-linear term

$$K_l < 1.4\times 10^{-8} \text{ meV cm} .$$

Maier *et al.*[12] give an upper limit of $K_1 < 10^{-7}$ meV cm which they derive from magnetoreflection measurements.

B. CdTe

The exciton binding energy of CdTe is much smaller than that of ZnTe. Therefore the $2P$-exciton structures are partially blotted out by the tail of the continuous absorption. Nevertheless in our best samples we could resolve the $2P$ structures even in the field-free case (Fig. 4). In an external magnetic field the two-photon oscillator strength of the P states is enhanced drastically. Figure 5 shows the magnetic field dependence of the state $|M_F=\frac{5}{2}, M_S=-\frac{1}{2}\rangle$. The solid line is the theoretical dependence calculated by Eq. (12). Experiment and theory are fitted at 6 T. In Fig. 6 the spectra for all eight polarization combinations of Faraday and Voigt configurations at 7 T are shown. The magnetic field dependence of the peak positions is shown in Fig. 7. The solid lines represent the eigenvalues which are calculated with the use of the following parameter set:

$$m_e^*=(0.099\pm0.003)m_0, \quad E_g=1.6063\pm0.0002 \text{ eV} ,$$

$$\gamma_1=4.11\pm0.15, \quad g_c=-2.2\pm0.5 ,$$

$$\gamma_2=1.08\pm0.15, \quad x=0.35\pm0.10 ,$$

$$\gamma_3=1.95\pm0.20, \quad q=0.0\pm0.1 ,$$

$$R_{\text{eff}}=9.5\pm0.2 \text{ meV} ,$$

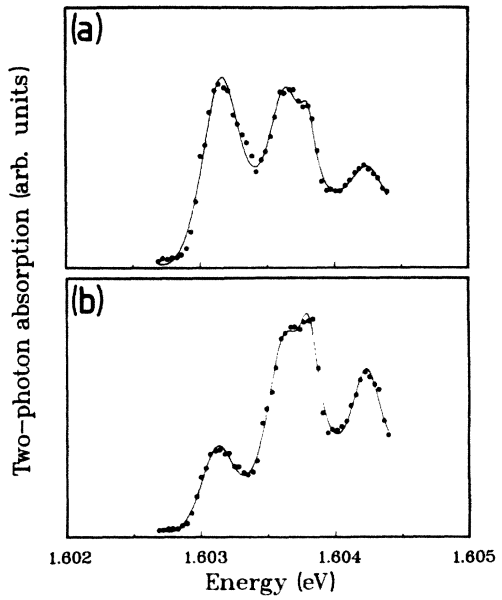

FIG. 4. Two-photon absorption spectra of the $2P$ exciton in CdTe for $B=0$ T. The solid lines are Lorentz oscillator fits to the experimental dots. (a) Polarization of the two lasers perpendicular to each other; (b) polarization of the two lasers parallel to each other.

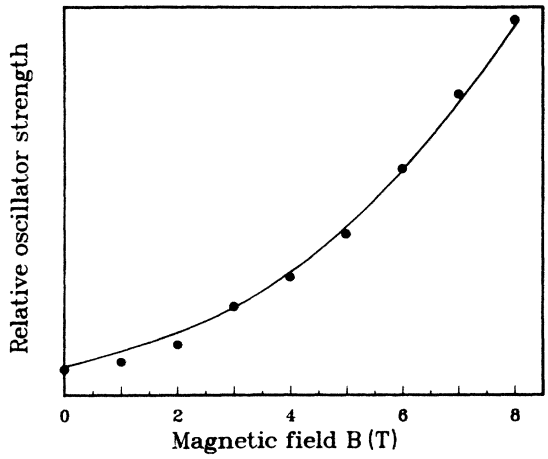

FIG. 5. Magnetic field dependence of the two-photon oscillator strength of the state $|M_F=\frac{5}{2}, M_S=-\frac{1}{2}\rangle$ in CdTe: line, theoretical calculation using the two-band model; dots, experimental results.

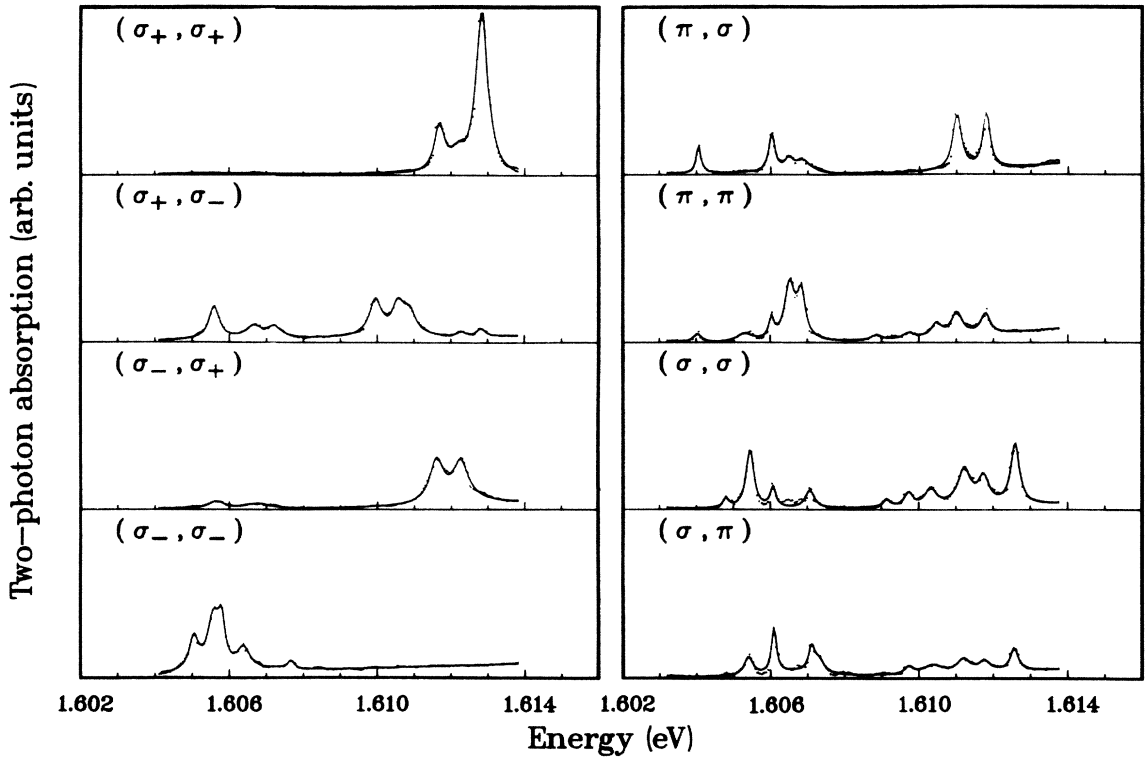

FIG. 6. 2*P*-exciton fine structure of CdTe at 7 T for the eight different polarization states of the two beams in Faraday (left) and Voigt configurations (right). The first sign refers to the polarization of the dye laser, the second to the polarization of the TEA CO_2 laser. The polarization is defined with respect to the magnetic field.

For the calculation of the eigenvalues we used wave functions with angular momentum up to $L=5$, which yields sufficient accuracy.

The electron effective mass derived here is in agreement with the results of the cyclotron resonance measurements of Romestain and Weisbuch,[3] Dang *et al.*,[4] Kanazawa and Brown,[5] and Mears and Stradling.[6] The values of Knap *et al.*,[7] Helm *et al.*,[8] and Peeters and Devreese[9] are "bare" electron masses, also gained from cyclotron resonance measurements. Using their values for the polaron coupling constant their masses are also in good agreement with our result. Marple[17] derived a value of $m_e^*=0.11m_0$ from free-carrier Faraday rotation experiments and from the contribution of these free carriers to the dielectric susceptibility, but his value has a large experimental error in comparison with our result. The cyclotron resonance of holes was investigated by Romestain and Weisbuch[3] in the [110]-direction. These measurements were extended to the [111] and [001] directions by Dang *et al.*[4] The heavy-hole masses differ from those calculated with our parameter set. Especially the anisotropy which they derive from their measure-

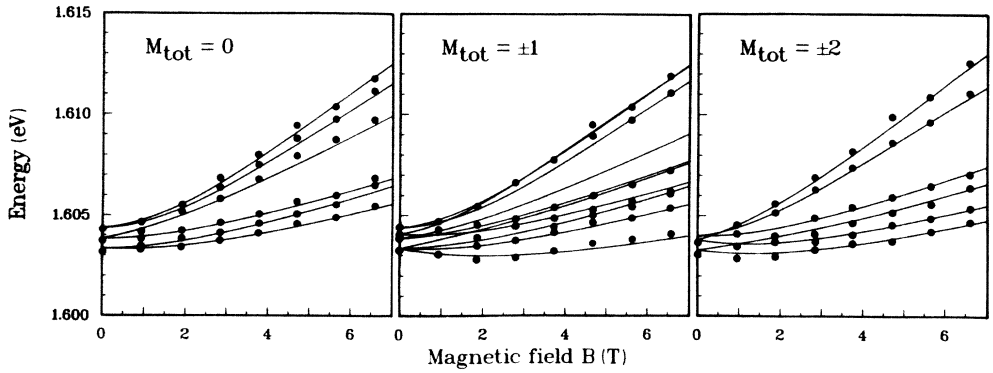

FIG. 7. Magnetic field dependence of the 2*P* multiplet in CdTe: lines, results of the calculations; dots, experimental peak positions.

TABLE III. Fundamental parameters of CdTe.

	m_e^*/m_0	γ_1	γ_2	γ_3	R_{eff} (meV)	g_c	κ	q
This work	0.099	4.11	1.08	1.95	9.5	−2.2	0.35	0.0
Romestain and Weisbuch[a]	0.096							
Dang *et al.*[b]	0.094	4.6	1.6	1.8				
Kanazawa and Brown[c]	0.096							
Mears and Stradling[d]	0.0965							
Knap *et al.*[e]	0.092							
Helm *et al.*[f]	0.090							
Peeters and Devreese[g]	0.092							
Marple[h]	0.11							
Molva and Dang[i]						−1.77	0.31	−0.02
Nakamura *et al.*[j]						−1.59		
Simmonds *et al.*[k]						−1.6		

[a] Reference 3.
[b] Reference 4.
[c] Reference 5.
[d] Reference 6.
[e] Reference 7.
[f] Reference 8.
[g] Reference 9.
[h] Reference 17.
[i] Reference 36.
[j] Reference 37.
[k] Reference 38.

ments is much smaller. But the heavy-hole resonances are rather broad and asymmetric so that a greater value of the anisotropy cannot be excluded by their experiment. The results of the different authors are compiled in Table III.

C. GaAs

In GaAs the exciton binding energy is only about 4 meV. Because of this small binding energy the $2P$ excitons are completely blotted out by the tail of the continuous absorption. In the field-free case only an unstructured increase of the two-photon absorption can be detected. This behavior is shown in Fig. 8. Because of the smaller masses and the smaller exciton binding energy the enhancement of the two-photon oscillator strength due to the magnetic field is even larger than in CdTe. The oscillator strength at 6 T is 30 times the oscillator strength at 0 T. This behavior is shown in Fig. 9 for the state $|M_F=\frac{5}{2}, M_S=-\frac{1}{2}\rangle$. Because of this enhancement we could detect distinct exciton lines in magnetic fields above 3 T. Figure 10 shows the spectra for the polarization combinations of the Faraday configuration. The linewidth of the exciton lines in GaAs is about four times the linewidth of the exciton lines in CdTe, which is the reason for the fact that we are not able to resolve all substates of the $2P$ multiplet. We have not performed measurements in Voigt configuration because the oscillator strength of the states in Voigt configuration is much smaller than in Faraday configuration. Measurements in Voigt configuration are only useful with better samples. Consequently we have fewer experimental data than in the case of ZnTe and CdTe to determine the mass parameters and g values. For this reason we have taken the parameters m_e^*, g_c, and q from other authors. The electron effective mass $m_e^*=0.066\,50m_0$ was determined very precisely by Fetterman *et al.*[11] from cyclotron resonance measurements. For the g values g_c and q we chose the result of Bimberg.[14] He derived $g_c=-0.44$ and $q=0.01$ from magnetoreflection data. We have determined the other parameters by fitting the theoretical eigenvalues to the experimental points. For the calculation of the eigenvalues we have included wave functions with angular momentum up to $L=7$. The following set gives the best fit to the experiment:

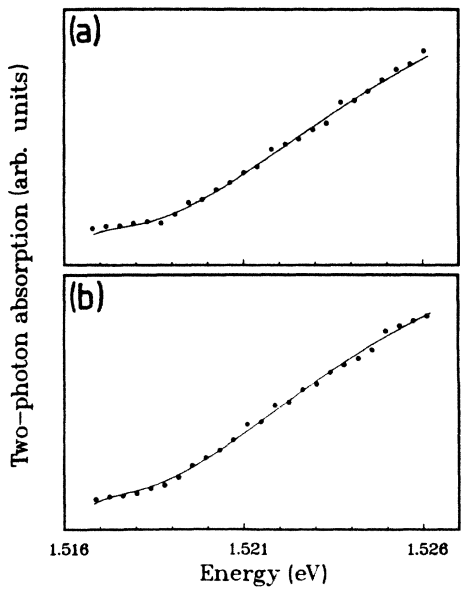

FIG. 8. Two-photon absorption spectra at the fundamental band edge of GaAs for $B=0$ T: (a) both lasers right circularly polarized; (b) dye laser, right circularly polarized; CO_2 laser, left circularly polarized.

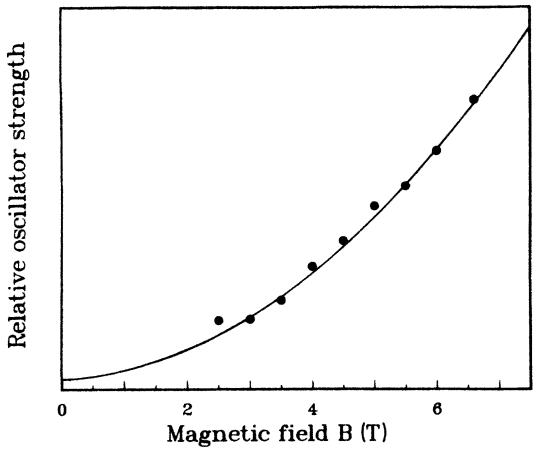

FIG. 9. Magnetic field dependence of the two-photon oscillator strength of the state $|M_F=\frac{5}{2}, M_S=-\frac{1}{2}\rangle$ in GaAs: line, theoretical calculation using the two-band model; dots, experimental results.

$\gamma_1=7.17\pm0.15$, $\kappa=1.81\pm0.10$,

$\gamma_2=2.88\pm0.15$, $R_{\text{eff}}=3.9\pm0.2$ meV ,

$\gamma_3=2.91\pm0.20$, $E_g=1.5200\pm0.0002$ eV ,

The agreement of experiment and theory is quite satisfactory, as shown in Fig. 11. One point of uncertainty in the above parameter set is that we had to take some of the parameters from other experiments. Another point is that we do not see any structure in the field-free case; therefore the determination of the anisotropy is difficult. It would be desirable to have better samples where the exciton lines have a smaller linewidth. Then we would be able to determine the complete parameter set for GaAs as well. A comparison of our values with the results of other authors is listed in Table IV. In general there is an agreement with the data of the other authors except that our data give a smaller anisotropy.

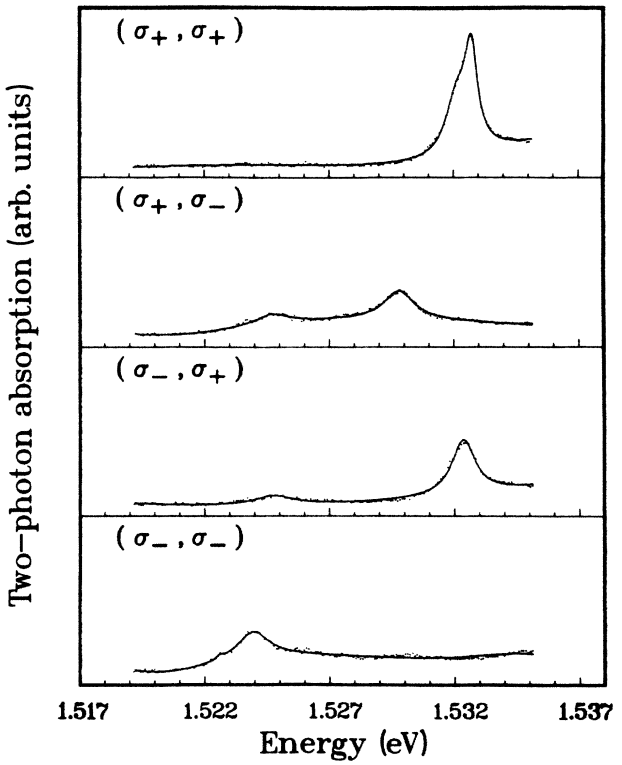

FIG. 10. 2*P*-exciton fine structure of GaAs at 6 T for the four different polarization states in Faraday configuration.

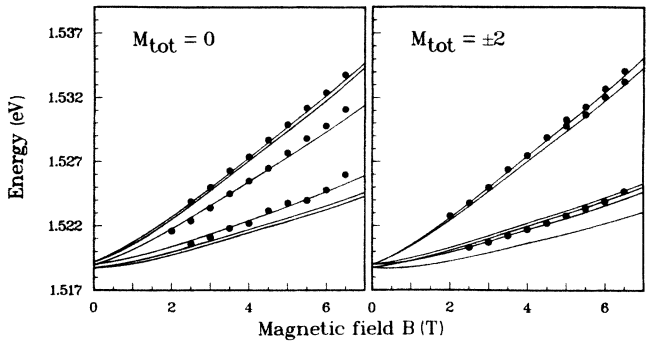

FIG. 11. Magnetic field dependence of the 2*P* multiplet in GaAs: lines, results of the calculations; dots, experimental peak positions.

V. SUMMARY

The 2*P* exciton system of zinc-blende-type semiconductors is characterized by a high orbital and spin degeneracy, which is lifted by an external magnetic field. The Zeeman splitting is highly nonlinear and depends very sensitively on the masses and *g* values of the conduction and valence bands. For the analysis of the *P*-exciton spectra we do not have to take into account exciton-phonon interaction, exciton-photon interaction, and central-cell corrections, which are all important for the analysis of *S*-exciton spectra. This fact simplifies the analysis of the 2*P*-exciton spectra considerably. Because of the critical dependence on the parameters and the straightforward analysis, the investigation of *P* excitons is an excellent method for the precise determination of

TABLE IV. Fundamental parameters of GaAs.

	γ_1	γ_2	γ_3	R_{eff} (meV)	κ
This work	7.17	2.88	2.91	3.9	1.81
Vrehen[a]	7.2	2.5	2.5		1.1
Bimberg[b]	6.85	2.1	2.9		1.2
Seisyan *et al.*[c]	7.1	2.32	2.54		
Skolnick *et al.*[d]	6.98	2.2	2.84		

[a] Reference 15.
[b] Reference 14.
[c] Reference 16.
[d] Reference 10.

band parameters and g values. Owing to the compression of the wave function in an external magnetic field the oscillator strength of P-excitons is enhanced drastically. Therefore, in magnetic fields pronounced $2P$-exciton structures can be seen even in materials where the higher excitons are not seen in the field-free case.

ACKNOWLEDGMENTS

The authors are grateful to Professor D. Fröhlich for his continuous support of this work. We acknowledge the financial support of this project by the Deutsche Forschungsgemeinschaft (Bonn, Germany).

[1]B. Clerjaud, A. Gelineau, D. Galland, and K. Saminadayar, Phys. Rev. B **19**, 2056 (1979).
[2]R. A. Stradling, Solid State Commun. **6**, 665 (1968).
[3]R. Romestain and C. Weisbuch, Phys. Rev. Lett. **45**, 2067 (1980).
[4]Le Si Dang, G. Neu, and R. Romestain, Solid State Commun. **44**, 1187 (1982).
[5]K. K. Kanazawa and F. C. Brown, Phys. Rev. **135**, A1757 (1964).
[6]A. L. Mears and R. A. Stradling, Solid State Commun. **7**, 1267 (1969).
[7]W. Knap, M. Helm, R. Lassnig, E. Gornik, and R. Triboulet, Acta Phys. Pol. A **67**, 171 (1985).
[8]M. Helm, W. Knap, W. Seidenbusch, R. Lassnig, E. Gornik, R. Triboulet, and L. L. Taylor, Solid State Commun. **53**, 547 (1985).
[9]F. M. Peeters and J. T. Devreese, Physica B + C **127B**, 408 (1984).
[10]M. S. Skolnick, A. K. Jain, R. A. Stradling, J. Leotin, J. C. Ousset, and S. Askenazy, J. Phys. C **9**, 2809 (1976).
[11]H. R. Fetterman, D. M. Larsen, G. E. Stillman, and P. E. Tannenwald, Phys. Rev. Lett. **26**, 975 (1971).
[12]W. Maier, G. Schmieder, and C. Klingshirn, Z. Phys. B **50**, 193 (1983).
[13]H. Venghaus and B. Jusserand, Phys. Rev. B **22**, 932 (1980).
[14]D. Bimberg, in *Advances in Solid State Physics,* edited by J. Treusch (Vieweg/Pergamon, Braunschweig, 1977), Vol. XVII, p. 195.
[15]Q. H. F. Vrehen, J. Phys. Chem. Solids **29**, 129 (1968).
[16]R. P. Seisyan, M. A. Abdullaev, and V. D. Draznin, Sov. Phys.—Semicond. **7**, 552 (1973).
[17]D. T. F. Marple, Phys. Rev. **129**, 2466 (1963).
[18]S. Nakashima, T. Hattori, P. E. Simmonds, and E. Amzallag, Phys. Rev. B **19**, 3045 (1979).
[19]H. W. Hölscher, A. Nöthe, and Ch. Uihlein, Phys. Rev. B **31**, 2379 (1985).
[20]Ch. Uihlein and S. Feierabend, Phys. Status Solidi B **94**, 153 (1979); *ibid.* **94**, 421 (1979).
[21]N. O. Lipari and M. Altarelli, Solid State Commun. **33**, 47 (1980).
[22]M. Cardona, N. E. Christensen, and G. Fasol, Phys. Rev. Lett. **56**, 2831 (1986).
[23]N. O. Lipari and A. Baldereschi, Phys. Rev. Lett. **25**, 1660 (1970).
[24]A. Baldereschi and N. O. Lipari, Phys. Rev. B **8**, 2697 (1973); *ibid.* B **9**, 1525 (1974).
[25]M. Altarelli and N. O. Lipari, Phys. Rev. B **9**, 1733 (1974).
[26]N. O. Lipari and A. Baldereschi, Solid State Commun. **25**, 665 (1978).
[27]A. R. Edmonds, *Angular Momentum in Quantum Mechanics* (University Press, Princeton, NJ 1960).
[28]H. J. Mattausch and Ch. Uihlein, Phys. Status Solidi B **96**, 189 (1979).
[29]G. D. Mahan, Phys. Rev. **170**, 825 (1968).
[30]R. J. Elliott, Phys. Rev. **108**, 1384 (1957).
[31]Ch. Neumann and A. Nöthe, Europhys. Lett. **4**, 351 (1987).
[32]D. Fröhlich, A. Nöthe, and K. Reimann, Phys. Status Solidi B **125**, 653 (1984).
[33]P. J. Dean, H. Venghaus, and P. E. Simmonds, Phys. Rev. B **18**, 6813 (1978).
[34]R. E. Nahory and H. Y. Fan, Phys. Rev. Lett. **17**, 251 (1966).
[35]M. Vanecek and E. Klier, Phys. Status Solidi A **30**, 441 (1975).
[36]E. Molva and Le Si Dang, Phys. Rev. B **32**, 1156 (1985).
[37]A. Nakamura, D. Paget, C. Hermann, C. Weisbuch, G. Lampel, and B. C. Cavenett, Solid State Commun. **30**, 411 (1979).
[38]P. E. Simmonds, H. Venghaus, R. Sooryakumar, and P. J. Dean, Solid State Commun. **43**, 311 (1982).